THE HIGH TEMPERATURE RAMAN SPECTROSCOPY AND ION CLUSTER THEORY FOR METALLURGICAL SLAG AND MAGMA

Guo-Chang Jiang, Yong-Quan Wu & Jing-Lin You
Shanghai University, China

ABSTRACT

This paper presents the high temperature Raman spectroscopy and corresponding ion cluster theory of molten silicates, i.e., metallurgical slag and geological magma. The Raman spectra were measured in situ using the high temperature Raman spectrometer with the spatial and accumulated time resolution techniques. The theoretical vibrational spectra were calculated from the silicate microstructure through so-called SiOT model. Finally, thermodynamic properties were calculated from the microstructure derived from the Raman spectra using a constructed thermodynamic CEMS model.

Key Words: *Raman spectra, Ion cluster theory, silicate, and thermodynamics.*

INTRODUCTION

Generally, the microstructure of a material is settled on its composition, and subsequently the properties of a material are rooted in their relationship with the microstructure. The effects of chemical potential on microstructure are attributed to the thermodynamic phenomena; however, viscosity, surface tension and diffusion coefficient are behaviors resulted from other effects on microstructure. In order to reveal the essential regularities of those important thermodynamic or kinetic properties as well as the inherent relations between or among those different properties, the unique way is to make it clear that how the microstructure changes and how the properties changes with the change of microstructure.

HIGH TEMPERATURE RAMAN SPECTROSCOPY (HTRS)

The high temperature Raman spectroscopy (HTRS) is one of the most efficient approaches in the research of microstructure of molten metallurgical slag and magma. Essentially, Raman spectrum reflects the vibration modes of an ion cluster in its micro environment. For silicates, the elementary microstructural units (clusters) are totally 5 kinds of Si-O tetrahedra (Q_n, n = 0~4) where n represents the number of bridging oxygen in one Si-O tetrahedron. From Figure1, people can recognize what kinds of Q_n are coexisted in a sample according to their micro- chemical potentials, or so-called the Raman shifts of the partial peaks after deconvolution, and the abundance of each existed Q_n according to the intensity of its peak. So the information resulted from Raman spectrum is comprehensive, even though it is not straightforward. Accordingly, we deduced a thermodynamic model to calculate the free energy directly based on the analytic data of Raman shift and Raman intensity and we will introduce it later. Here in this section, the HTRS is firstly introduced especially some key techniques in order to weaken or eliminate the high temperature effect.

The first difficulty in running HTRS is that the thermal emission is increased as a function of T^4 meanwhile the Raman intensity is decreased following the temperature rising, which means the signals of Raman scattering are all submerged in the thermal noise while high temperature. So far several HTRS approaches were developed to suppress strong thermal emission and to ensure a high enough ratio of signal to noise. Among them the approach following either spatial resolution or accumulated time resolution is successful. Using a confocal microscope to record Raman spectra is called micro Raman, and the spatial resolution is provided by the confocal microscope and two conjugated diaphragms in the light path. The full width of half maximum (FWHM) of the curve shown in Figure 2 equals the focus depth associating with the operation parameters. If the objective is of 50× when the pinhole diameter of the diaphragm fitted on imaging platform is enlarged from 50 μm to 300 μm the focus depth is increased by 30% (from 20 μm to 28 μm) as shown in Figure2. This means the thermal emission is enlarged by 30% but the Raman intensity is by 6-fold of the original. So the cost to compensate the enhancement of spatial resolution effectiveness is an obvious decrease of the Raman intensity. Namely, in the case of spatial resolution the inhibition of thermal emission is in contradiction to ensure a high enough ratio of Raman signal to noise.

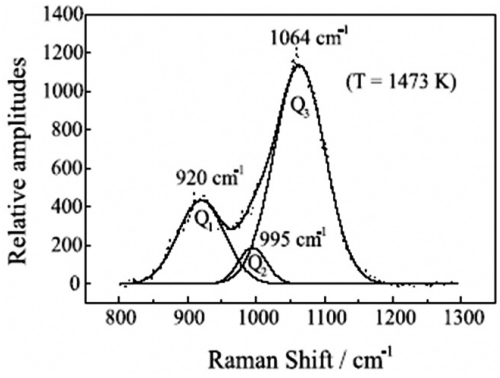

Figure 1: Spectral deconvolution of symmetric stretching vibrational envelop for Raman spectra of $Na_2O{\cdot}2SiO_2$ melt at 1473 K

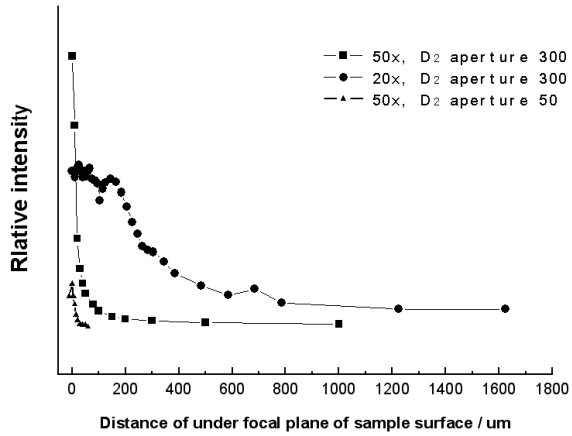

Figure 2: The intensity variation of 465 cm^{-1} peak of quartz crystal vs. the horizontal of sample surface

In a HTRS following an accumulated time resolution principle a pulsed laser is used instead of continuous laser in inducing Raman signal. The transient intensity of a pulse is much stronger than the rated power of laser source, so the energy density on the focus is increased a lot if a pulsed laser is adopted. The stronger the incident is, the more intense the scattering is.

On the other hand, the magnitude of time constant for Raman scattering detection τ_{RS} is of 10^{12}, that for pulsed laser τ_p is of 10^9 and that for noise is infinitive. Figure 3 elucidates this situation. One can see that the thermal emission in the whole time interval between two pulses, but the Raman scattering signal induced by a pulse extends only for $4\tau_{RS}$ after the end of the pulse. This brings the possibility to separate the signal and thermal emission successfully.

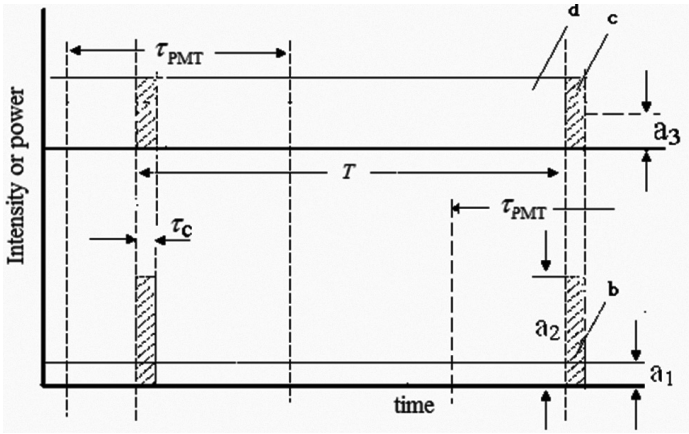

a1) the rated power of the laser source,	b) the Raman scattering induced by one pulse
a2) the transit power of the incident pulse,	c) the recorded thermal emission
a3) the averaged power of thermal emission,	d) the rejected thermal emission

Figure 3: The illustration of accumulated time principle

Coupling with pulsed laser, a HTRS following the accumulated time resolution principle adopts a coincidence circuit to control spectrum record. At every moment when the pulsed Raman signal emerges this circuit is closed once a time. The window time of once a closure is $\tau_C = \tau_p + 4\tau_{RS} \approx 10$ns. So the pulsed Raman signal and the thermal emission or blackbody radiation in this short window time are recorded. All the thermal emission in the interval of ~10^5ns (=T- τ_C, T is the cycle of the pulse) is rejected. Thus integrating many times the records makes the spectrum having a ratio of signal/background of (T/τ_C) times over the original ratio.

If a continuous laser is used to record the spectrum, the function of *F(T)* is shown by curve *a* in Figure 4, which shows when the thermal emission from background does not to be rejected and the temperature limit is lower than 1400 K. Actually in recording spectrum following spatial resolution principle for a temperature above 1500 K, the thermal emission irradiating from the volume of spatial focus is impossible to be omitted. By means of a special correction suggested to offset the effect of thermal emission on the originally recorded spectrum, the working temperature of a spatial resolution HTRS can reach 1773~1873 K. If using accumulated time resolution principle, the recorded intensity of the thermal emission of background is decreased by *K* times. $K = (f\tau_C)^1$, f is the pulse repeating frequency. The curve *b* in Figure 4 corresponds with K=3000, so the temperature limit is up to 2500 K. But in fact the thermal emission is of 10^4 - fold, so the limit can reach 2700~2900 K or higher. In addition, one should notice that the temperature limit is also possible to be effected by the Raman response of the sample.

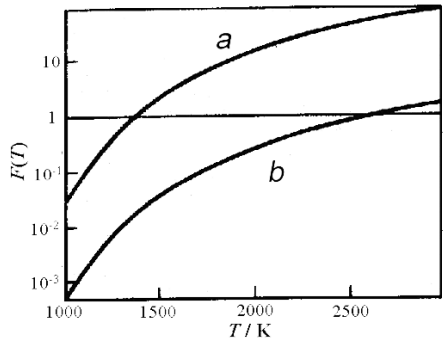

Figure 4: The variation of function $F=Ip(\Delta\nu)/10\delta_b$ following temperature

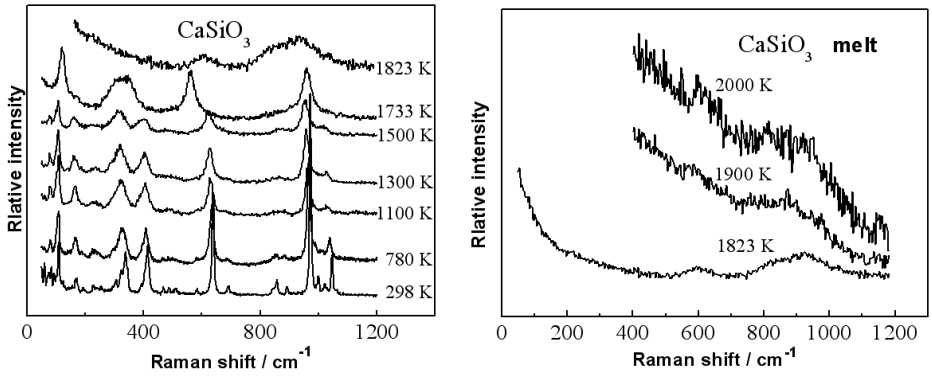

Figure 5: The Raman spectra of β-$CaSiO_3$ at diverse temperatures

Figure 5 displays the Raman spectra of β-$CaSiO_3$ at diverse temperatures. Thanks to the spatial and time resolution principles, the spectra of $CaSiO_3$ for the whole temperature range from solid to liquid were achieved. Obviously the spectrum of crystal is some sharp line-like peaks. Following temperature is elevated the FWHM of the peaks become wider and wider. From 1733 K to 1823 K the spectrum behaves as an envelope, this agrees well with the melting point of $CaSiO_3$, 1819 K.

It was stipulated when recording the spectra in Figure 5 that after raising temperature once a time the sample should be isothermally kept for 1h in general before recording the spectrum. According to phase diagram, the phase transition from β-$CaSiO_3$ to α-$CaSiO_3$ happens at 1398 K. But it was found by the present authors that after keeping the sample isothermally at 1400 K for 5 h the transition does not finished. Even up to 1500 K the spectrum shown in Figure 5 does not exhibit clearly the trace of transition. Only the spectra over 1733 K exhibit the transition to α-$CaSiO_3$. This is a typical instance to elucidate that the transformation of microstructure is frequently retarded a lot in comparison with the change of temperature. The lower the temperature is, or the larger the viscosity of a melt is, the longer isothermally keeping time is needed to finish the transformation of microstructure. For HTRS what is the appropriate isothermally keeping time for a definite sample to finish the microstructural relaxation can be determined and the temperature is a knowhow.

As McMillan *et al.* [1] claimed, the relaxation time of the microstructure of silicates is closely associated with the composition and the temperature. A temperature high as 5000 K is demanded for a silicate with low viscosity to have a fast enough relaxation, and

for quartz, maybe 10000 K is a must. If the isothermally keeping time is not long enough, the phase transformation will start to emerge from a temperature higher than the critical temperature and finish at a temperature far from the critical. Zu *et al.* [2] studied a molten In20Sn80 alloy by means of HT-XRD, the melting point of the alloy is 468 K. They found that the thermal insulating time should be 2h when the experiment was carried out at 573 K. If it was 853~1173 K, 30 min was appropriate.

Thus, in the case of a lower temperature and a shorter thermal insulating time, it is impossible to attribute the recorded spectrum to a definite temperature reliably. For the Strict remarks to really understand the microstructure of molten silicate, following three items should be satisfied simultaneously.

- The measurement must be carried out directly in molten state
- If the spectra measured both in heating and cooling processes coincides with each other, the spectra are doubtlessly the best result. The first thing to get a creditable spectrum is a long enough isothermally keeping time for the sample preparation after change temperature once a time in either a heating process or a cooling process
- In order to check the repeatability of the results the thermal history of all samples must be the same.

In Shanghai University, two sets of HTRS instruments were established. They are able to record spectra at 2000 K or higher. The newer system combines the principles of accumulated time resolution and spatial resolution. It is composed of a pulse laser generator, a micro-Raman system and an ICCD, which makes the system capable to work in the case of UV or VIS.

ION CLUSTER THEORY

Based on the experimental condition of HTRS, we also constructed a theoretical system for the metallurgical slags and magma to interpret the vibrational source for Raman spectra and to connect the macro thermodynamics with the proved microstructural data.

The 5 kinds of Si-O tetrahedra (Q_n , n=0,1,2,3,4) are the simplest ion cluster in metallurgical molten slags and magma. They are considered to be the basic microstructural units in SiOT model introduced by Wu *et al.* [1]. At first, the spatial coordinates of more than 250000 Q_n for every slag sample are generated by means of molecular dynamics simulation. The EVA (eigen vibration analysis) of these tetrahedra is performed along with GF matrix method. Based on the eigen vectors resulted from EVA, the Raman scattering intensity of partial spectra of each kind of Q_n is calculated according to EOP (electro-optical parameters method) and BPM (bond polarizability model). Finally, summarizing all the partial spectra comes to the results of final envelope. The unique merit of SiOT model is that it can describe the distribution of cluster vibrational behaviors in a system according to the distribution of microstructural units and their distortion coming from their various local surroundings.

Figure 6 displays the MD simulated results of 6 samples of $CaO\text{-}SiO_2$ system with the composition varying from O/Si=2.5 to O/Si=5 plus the reference system of pure SiO_2, which is in good agreement with several experimental results of literatures [3]. This is an evidence of the Si-O network in molten silica and silicates.

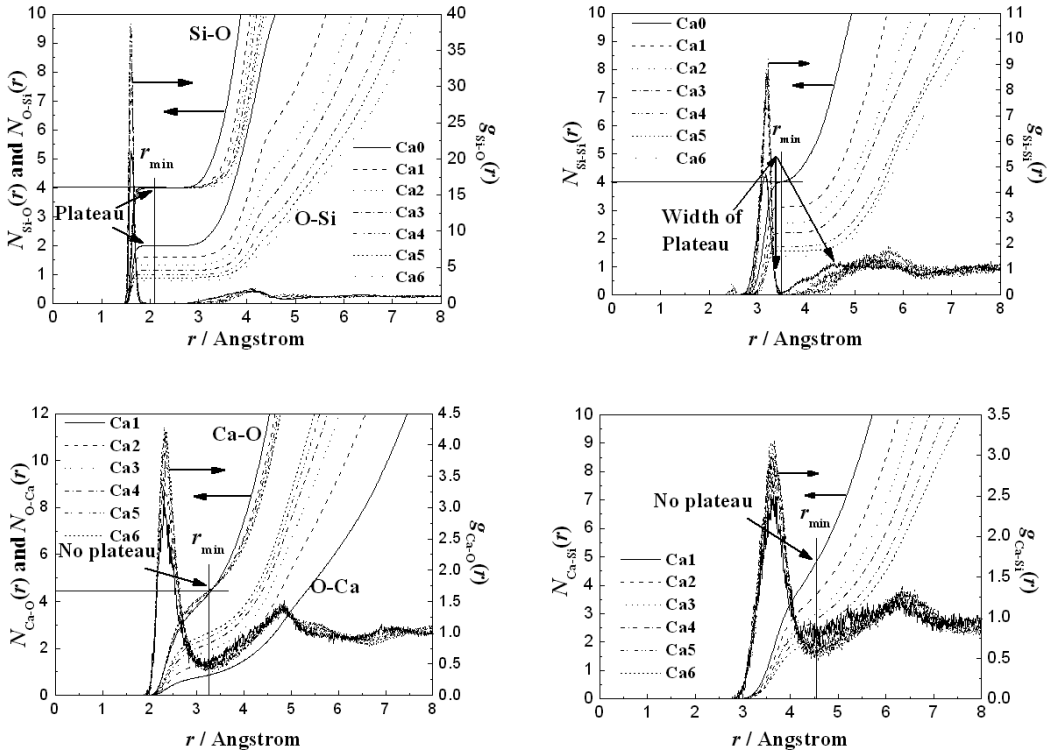

Figure 6: The MD simulated RDF (Radial Distribution Function) and CN (Coordination Number) of CaO-SiO_2 system

In a silicate crystal, one kind of Q_n is usually contained. But in a silicate glass or melt, several kinds of Q_n might be co-existed. The feature of molten silicate spectra is the emergence of the envelope, as shown in Figure 5. It hints that in melt the co-existed kinds of Q_n could be up to 5. And the interaction among them obeys the following converting reaction.

$$2Q_n = Q_{n-1} + Q_{n+1} \quad (1)$$

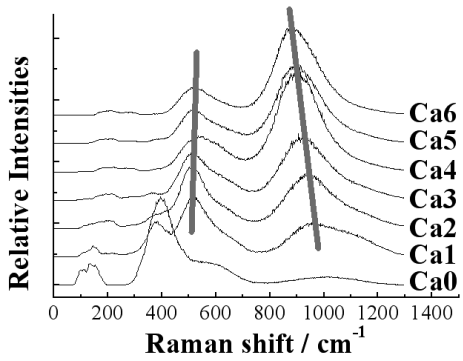

Figure 7: Effect of composition on the spectra of melts. The compositions of the samples coincide with the samples of Figure 6

The variation of Raman envelope caused by the change of composition in molten CaO-SiO_2 slag, as a result of MD simulation in Figure 6, is displayed in Figure 7. The lower

frequency shift of envelope in high wavenumber region indicates that variation tendency of $Q_4 \rightarrow Q_3 \rightarrow Q_2 \rightarrow Q_1 \rightarrow Q_0$ due to the restraint of the mentioned converting reaction.

Raman spectrum comes from molecular vibration. The Raman shift of a partial peak is determined by the relevant vibration mode. For example, the SS (symmetrical stretch) mode of O_{nb} for Q_2 as shown in Figure 8 is the first factor deciding the peak position in high wavenumber region. On the other hand, the span of every partial Raman peak is some tens of wavenumber. This means in each kind of Q_n, the frequency of SS mode of O_{nb} has a distributing regularity. Two tetrahedrons of same kind located in different micro environment may have different bond lengths and bond angles. That's to say, in every kind of Q_n, bond length and bond angle have also a distributing regularity, and the micro chemical potential of a Q_n is just dependent on that. The SiOT model may correctly describe the distributing regularity because it bases on the statistics of the configuration of 250000 or more Q_n in space.

SiOT model provides the information of $\sum_n$, which is the Raman scattering coefficient or the relative scattering cross section of Q_n.

$$(Q_n)_{\text{Mole}}\% = A_n / \sum_n \tag{2}$$

An denotes the area covered by the partial Raman peak. It was found earlier by many researchers that the $\sum_n \neq \sum_{n-1}$, because different Q_n contains different amount of O_{nb} (non-bridging oxygen). Some of $\sum_n$ in Na_2O-SiO_2 system was measured at room temperature [7, 8], however, so far no way to directly detect $\sum_n$ for molten state due to lack of suitable standard sample. It can be seen that according to SiOT model the averages of $\sum_n$ is independent for temperature and composition. For molten CaO-SiO_2 slag, the average $\sum_n$ calculated from SiOT model is fitted as:

$$\sum_n = 0.08749 + 1.09074 \exp(-\frac{n}{1.69937}) \tag{3}$$

For molten Na_2O-SiO_2 slag, that is $\sum_0$=1, $\sum_1$=0.514, $\sum_2$=0.242, $\sum_3$=0.09, $\sum_4$=0.004 and

$$\sum_n = 0.09849+1.10472\exp(-\frac{n}{1.69774}) \tag{4}$$

So the same $\sum_n$ for two kinds of slag are different, which is attributed to the network modification effect of different cations.

Following SiOT model, the CEMS model (cluster equilibrium of molten silicates or metallurgical slags) has been developed also, which is used to link ion cluster and thermodynamic properties in equilibrium state (as mixing free energy) [3]. According to CEMS model, X denotes mole fraction. M^{2+} is not included in Q_0, Q_1, Q_2, Q_3. If n denotes molar amount, then the free energy of the system of $[\sum_{i=0}^{4} n_i + n_M + n_O] = 1$ is:

$$G = \left(\sum_{i=0}^{4} X_i H_{i,mol} - T \sum_{i=0}^{4} X_i S_{i,mol}^{ncf} - TS^{cf} \right) \tag{5}$$

Which includes three parts of contributions: enthalpy $H_{i,mol}$, non-configurational entropy $S_{i,mol}^{ncf}$, and configurational entropy S^{cf}. The configurational entropy S^{cf} is deduced according to the idea of two-lattice model as

$$
\begin{aligned}
-\frac{S^{config}}{R} = & -\left(2\sum_{i=0}^{4}X_i + X_O\right)ln\left(2\sum_{i=0}^{4}X_i + X_O\right) + X_O \ln X_O \\
& + \sum_{i=0}^{3}\left(\frac{((4-i)X_i)^2}{2\sum_{i=0}^{3}(4-i)X_i}ln\frac{((4-i)X_i)^2}{2\sum_{i=0}^{3}(4-i)X_i}\right) + 2\sum_{\substack{i=0\\j=0\\i\neq j}}^{3}\left(\frac{(4-i)X_i(4-j)X_j}{2\sum_{i=0}^{3}(4-i)X_i}ln\frac{(4-i)X_i(4-j)X_j}{2\sum_{i=0}^{3}(4-i)X_i}\right) \\
& + \sum_{i=1}^{4}\left(\frac{(iX_i)^2}{2\sum_{i=1}^{4}iX_i}ln\frac{(iX_i)^2}{2\sum_{i=1}^{4}iX_i}\right) + 2\sum_{\substack{i=1\\j=1\\i\neq j}}^{4}\left(\frac{iX_i jX_j}{2\sum_{i=1}^{4}iX_i}ln\frac{iX_i jX_j}{2\sum_{i=1}^{4}iX_i}\right)
\end{aligned}
\tag{6}
$$

The evaluations of enthalpy $H_{i,mol}$ and non-configurational entropy $S^{ncf}_{i,mol}$ as the relative properties of 1 mole Q_n are based on the standard enthalpies and entropies of several single crystals.

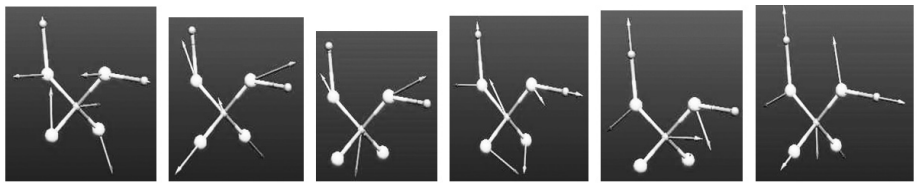

Figure 8: The eigen vibrational modes of Q_2

The process of making the integrated free energy under linear restriction close to its minimum is carried out through optimization according to external penalty function approach [3]. Meanwhile, the mole fraction of 5 Q_n (X_i) in equilibrium state can be determined. It is found from Figure 9 that the X_i calculated from CEMS model through optimization agrees well with the X_i accounted according to MD simulation as the first part of SiOT model.

The above discussion indicates that the entire information of 5 Q_n got from both HTRS measurement and SiOT model computation can be used as known knowledge for CEMS model. Figure 10 exhibits the computational result of mixing free energy in the whole composition range through the optimization mechanism of CEMS model. Actually, that's the outstanding feature of CEMS model. With the optimization mechanism, it can act as an independent structural thermodynamic model; and without the optimization mechanism and directly based on the information of Q_n obtained from experimental or theoretical spectra, it can act as a thermodynamic calculator.

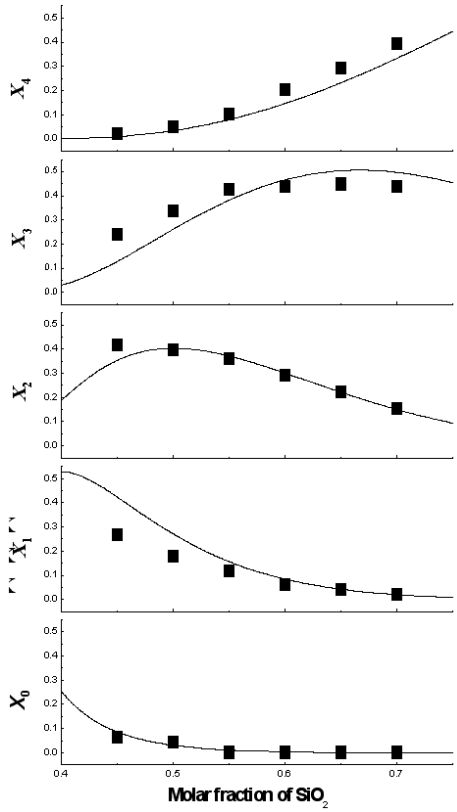

Figure 9: The comparison of X_i calculated by CEMS model (curve) and simulated by MD (■) for $\sum_{i=0}^{4} X_i = 1$

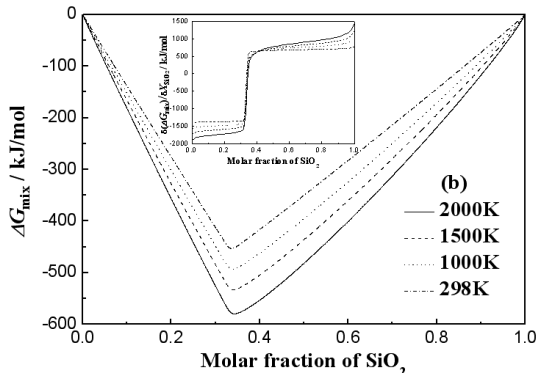

Figure 10: The mixing Gibbs free energy of ΔG_{mix} in the whole composition range according to the optimization mechanism of CEMS model

In SiOT model 5 kinds of Q_n in silicate are selected as the micro-structural units, so the problem is reduced to a description of the distribution of bond lengths and bond angles for Q_n. The entire information of microstructure of silicates including the mole fraction of Q_n and their micro-chemical potential can be achieved by integrating HTRS experiment and SiOT model. Then through CEMS model one can interconnect the thermodynamic properties of slag to their microstructures.

Tetrahedra are the smallest and simplest clusters in silicate. Based on tetrahedra to classify molten silicate is a reasonable approach even for the aluminosilicate system. When an Al ion enters into a Q_n of Si-O to replace the Si site, the effect can be recognized as the change of the micro-chemical potential of that Q_n. Then, the SiOT model and CEMS model can be expanded to the aluminosilicate system.

ACKNOWLEDGEMENTS

This work is supported by the State Key Program of the National Natural Science Foundation of China (Grant No. 50334040), the Program of the National Natural Science Foundation of China (Grant No. 50504010), the Joint Funds of the National Natural Science Foundation of China and Shanghai Baosteel Corporation, China (Grant No. 50774112), the Qimingxing Program for Young Scientists of Shanghai, China (Grant No. 07QA14021) and the Program for Changjiang Scholars and Innovative Research Team in University (Grant No. IRT0739).

REFERENCES

McMillan, P. F., Wolf, G. H. & Poe, B. T. (1992). *Vibrational Spectroscopy of Silicate Liquids and Gasses*. Chem. Geo., 96: 351-366. [1]

Zu, F. Q., Zhu, Z. G., Guo, L. T., Qin, X. B., Yang, H. & Shan, W. J. (2002). *Observation of Anomalous Discontinuous Liquid Structure Change with Temperature*. Phys. Rev. Lett., 89: 105525. [2]

Wu, Y. Q. (2004a). *Theoretical Studies on the Micro-structure of Molten Silicates and its Relation with the Macro-properties*. PhD Thesis of Shanghai University. [3]

Wu, Y. Q., Jiang, G. C., You, J. L., Hou, H. Y., Chen, H., & Xu, K. D. (2004b). *Theoretical Study of the Local Structure and Raman Sectra of CaO-SiO_2 Binary Melts*. J. Chem. Phys., 121: 7883-7895. [4]

Waseda, Y. & Toguri, J. M. (1998). *The Structure and Properties of Oxide Melts: Application of Basic Science to Metallurgical Processing*. World Scientific Publishing Co. Ltd., Singapore, P21. [5]

Guyot, F., Wang, Y. B., Gillet, P. & Ricard, Y. (1996). *Quasi-harmonic Computations of Thermodynamic Parameters of Olivines at High-pressure and High-temperature*. A Comparison with Experiment Data, Phys. Earth Planet. In, 98:17-29. [6]

You, J. L., Jiang, G. C. & Xu, K. D. (2001). *High Temperature Raman Spectra of Sodium Disilicate Crystal*. Glass and its Liquid, J. Non-Cryst. Solids, 282: 125-128. [7]

Mysen, B. O. & Frantz, J. D. (1994). *Alkali Silicate Glass and Melt Structure in the Temperature Trange 25-1651 C at Atmospheric Pressure and Implications for Mixing Behavior of Structural Units*. Contrib. Mineral. Petrol., 117: 1-14. [8]

Zhang, P., Grandinetti, P. J. & Stebbins, J. F. (1997). *Anionic Species Determination in $CaSiO_3$ Glass Using Two-Dimensional 29Si NMR*. J. Phys. Chem. B, 101: 4004-4008. [9]

Seetharaman, S., Sichen, D. & Ji, F. Z. (2000). *Estimation of Viscosities of Ternary Silicate Melts using the Excess Gibbs Energy of Mixing*. Metall. Mater. Trans. B, 38 (1): 105-109. [10]